Bioorganic & Medicinal Chemistry Letters xxx (xxxx) xxx–xxx

Contents lists available at ScienceDirect

Bioorganic & Medicinal Chemistry Letters

journal homepage: www.elsevier.com/locate/bmcl

Discovery, synthesis and characterization of a series of (1-alkyl-3-methyl-1*H*-pyrazol-5-yl)-2-(5-aryl-2*H*-tetrazol-2-yl)acetamides as novel GIRK1/2 potassium channel activators

Swagat Sharma[a], Krystian A. Kozek[b,d], Kristopher K. Abney[c], Sushil Kumar[a], Nagsen Gautam[a], Yazen Alnouti[a], C. David Weaver[b,d], Corey R. Hopkins[a,*]

[a] Department of Pharmaceutical Sciences, College of Pharmacy, University of Nebraska Medical Center, Omaha, NE 68198-6125, USA
[b] Department of Pharmacology, Vanderbilt University School of Medicine, Nashville, TN 37232, USA
[c] School of Graduate Studies and Research, Meharry Medical College, Nashville, TN 37208, USA
[d] Vanderbilt Institute of Chemical Biology, Vanderbilt University, Nashville, TN 37232, USA

ARTICLE INFO

Keywords:
GIRK
G protein-regulated inwardly-rectifying potassium channel
Activator
Tetrazole

ABSTRACT

The present study describes the discovery and characterization of a series of 5-aryl-2*H*-tetrazol-3-ylacetamides as G protein-gated inwardly-rectifying potassium (GIRK) channels activators. Working from an initial hit discovered during a high-throughput screening campaign, we identified a tetrazole scaffold that shifts away from the previously reported urea-based scaffolds while remaining effective GIRK1/2 channel activators. In addition, we evaluated the compounds in Tier 1 DMPK assays and have identified a (3-methyl-1*H*-pyrazol-1-yl)tetrahydrothiophene-1,1-dioxide head group that imparts interesting and unexpected microsomal stability compared to previously-reported pyrazole head groups.

Introduction

G protein-gated inwardly-rectifying potassium channels (GIRK), also known as $K_{ir}3$, are a family of inwardly-rectifying potassium channels that are key effectors in GPCR signaling pathways that modulate excitability in cells.[1,2] In mammals, four GIRK channel subunits are expressed, GIRK1-4 ($K_{ir}3.1$–3.4), which form either homo- or heterotetramers.[3,4] GIRK1-3 are typically expressed in the brain, whereas GIRK4 is found in heart atria, where it plays a key role in regulating heart rate. Previous research supports roles for GIRK channels in a number of normal and pathophysiological processes, including pain perception,[5–7] epilepsy,[8–10] memory,[11] and reward/addiction.[12–14] Due to our interest in discovering novel targets and tool compounds for diseases of the brain, we have focused our efforts on the GIRK1/2 channel due to its localization in the CNS. However, due to a dearth of subunit-selective GIRK activators, efforts to investigate the potential benefits of GIRK channels in disease therapy have been hampered. Herein, we report a new and distinct scaffold that shows promise as a selective GIRK1/2 activator that we developed based on a molecule discovered from our initial high-throughput screening (HTS) campaign (See Fig 1).

We have previously reported on a series of urea-based GIRK1/2 activators (i.e., **1**); however, the utility of this series of compounds was limited by poor pharmacokinetic (PK) properties (low brain penetration and poor solubility).[8,10] From the urea-series, we scaffold-hopped to the phenylacetamide series, **2**,[15] which showed promise as a potent GIRK1/2 activator. Although this series of compounds was able to improve some pharmacokinetic properties (e.g., brain penetration), they suffered from poor metabolic stability as measured in human and mouse liver microsomes. Thus, we further investigated the compounds identified from a previous HTS campaign.[8] We were interested in a new, tetrazole containing scaffold, **3**. This represented an interesting and unique starting point for optimization because it did not contain the privileged pyrazole head group. Further, the phenyl tetrazole was curious because previous attempts to derivatize off the right side phenyl groups of **1** or **2** did not prove productive.[16,17] Herein, we report the synthesis, biological characterization, and *in vitro* PK properties of this new scaffold of GIRK1/2 activators.

Synthesis of the studied compounds started with the disubstituted pyrazole head group (e.g., **7**). For starting materials that were not commercially available, the synthesis outlined in Scheme 1A and B was followed. Namely, the appropriately-substituted ethyl ester, **4**, was reacted with acetonitrile (*n*-BuLi, THF, −78 °C to rt) yielding **5**.[15,17] This compound was then cyclized with the substituted hydrazine **6** under

* Corresponding author.
E-mail address: corey.hopkins@unmc.edu (C.R. Hopkins).

https://doi.org/10.1016/j.bmcl.2019.01.027
Received 19 November 2018; Received in revised form 21 January 2019; Accepted 22 January 2019

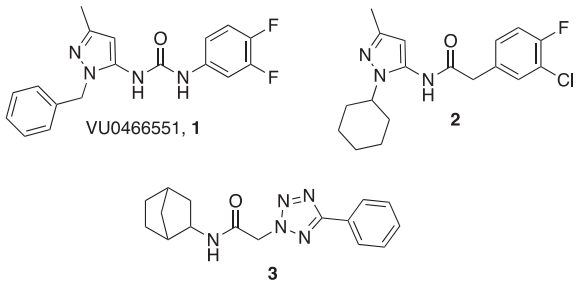

Fig. 1. Previously reported GIRK1/2 activators, **1** and **2**, and the new *N*-(bicyclo[2.2.1]heptan-2-yl)-2-(5-phenyl-2*H*-tetrazol-2-yl) acetamide, a starting lead for GIRK1/2 activator optimization.

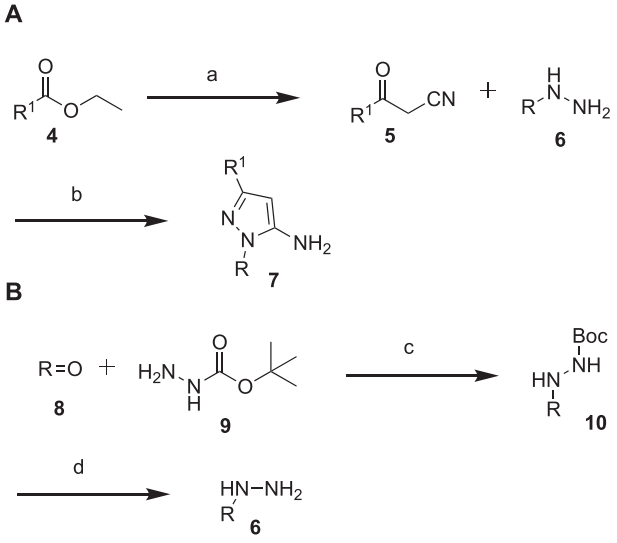

Scheme 1. Reagents and conditions: (a) CH_3CN, *n*-BuLi, THF, −78 °C to rt; (b) AcOH, EtOH, reflux; (c) $NaCNBH_3$, AcOH, MeOH, rt; (d) TFA, CH_2Cl_2, rt.

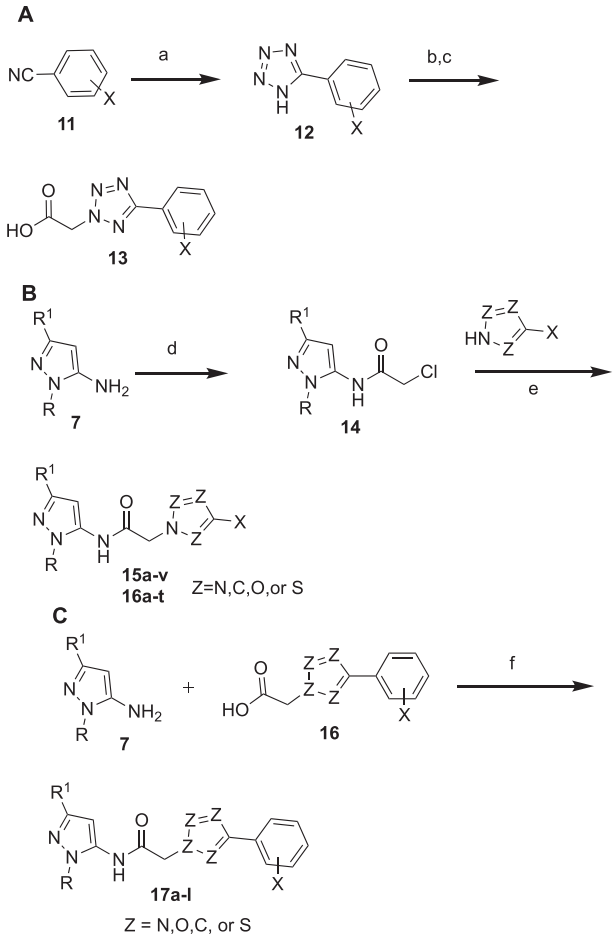

Scheme 2. Reagents and conditions: (a) NaN_3, Et_3N-HCl, toluene, 120 °C; (b) bromoethyl acetate, NaOEt, EIOH; (c) NaOH, H_2O, THF; (d) 2-chloroacetyl chloride, Et_3N, CH_2Cl_2; (e) NaOEt, EtOH, μW, 90 °C; (f) T3P, Et_3N, CH_2Cl_2, rt.

acidic conditions (AcOH, EtOH, reflux) to yield the desired disubstituted pyazoloamine, **7**. For those substituted hydrazines that were not commercially available, the synthetic procedure outlined in Scheme 1B was followed. The Boc-hydrazine, **9**, was reacted with the carbonyl, **8**, under reductive amination conditions ($NaCNBH_3$, AcOH, MeOH, rt) to yield **10**, which was subjected to TFA in order to remove the Boc protecting group and yield the desired hydrazine, **6**.[18]

The synthesis of the final tetrazole or heterocyclic compounds was completed as outlined in Scheme 2A–C. The tetrazole-containing compounds were synthesized by reacting the appropriately-substituted aryl cyanide with NaN_3 (Et_3N·HCl, toluene, 120 °C) to yield **12**.[19] Next, **12** was reacted with bromoethyl acetate (NaOEt, EtOH)[20] and followed by saponification of the ester (NaOH, H_2O, THF) to give the acid coupling partner, **13**. In an analogous fashion to the final targets, the disubstituted pyrazoloamine, **7**, was coupled with 2-chloroacetyl chloride (Et_3N, CH_2Cl_2) affording the α-chloroamide, **14**. This compound could then be reacted with a heterocyclic partner under basic conditions to yield the final targets, **15**. Also, the acid coupling partner (e.g., **13** or **16**) could be reacted with **7** under standard amide coupling procedures (T3P, Et_3N, CH_2Cl_2) to yield the final targets, **17**.[21]

The initial structure-activity relationship (SAR), which was centered around the left-hand amide portion, is detailed in Table 1. The initial HTS hit molecule was resynthesized and tested on HEK293 cells expressing GIRK channels using thallium flux assays, as previously described.[8] This molecule demonstrated weak activity against GIRK1/2 (**3**, EC_{50} = 1980 nM, Efficacy = 13% of a maximally effective concentration of VU0466551), which agreed with previous data showing non-pyrazole "head groups" to be weak GIRK1/2 activators. Using our knowledge from previous work, we attached the 3-methyl-1-cyclohexylpyrazole group to generate **15a**, which we found to be a potent and efficacious GIRK1/2 activator (EC_{50} = 96 nM; Efficacy = 92%). This compound was also a GIRK1/4 activator, but it demonstrated an approximate 3-fold preference for GIRK1/2. Methylation of the amide nitrogen led to an inactive molecule (data not shown). Moving from the amide to the thioamide, **15b**, produced an active molecule; however, we observed an approximate 7-fold loss of potency (EC_{50} = 623 nM). Further saturated 6-membered analogs were evaluated and the tetrahydropyran, **15c**, lost activity compared to **15a**. However, the 4,4-difluorocyclohexane was equipotent (**15d**, EC_{50} = 84 nM), but potency eroded with substituting dimethyl, **15e**, for the difluoro. Further branched alkyl analogs were less potent (**15f–h**), and the cyclopropyl was also inferior, but some activity could be regained with the cyclopentyl group (**15j**, EC_{50} = 163 nM). The 5- and 6-membered sulfone derivatives (**15k**, **l**) were also less active; however, these were shown to have superior *in vitro* PK properties (*vide infra*). Branched groups at the 3-position of the pyrazole were not productive analogs (**15m–p**). The 1-cyclohexylmethyl group, as we have seen previously, was an active analog (**15q**, EC_{50} = 176 nM); however, this molecule lost selectivity between GIRK1/2 and GIRK1/4. Other substituents (**15r**), or 5-membered pyrazole replacements (**15s, t**) were not active, nor were pyridine replacements for the pyrazole (**15v**).

We next set out to evaluate the right-hand phenyl group (Table 2). Replacement of the phenyl with either 3-pyridyl (**16a**) or 2-pyridyl (**16b**) led to a > 20-fold loss of activity. Addition of halogens (either mono- or di-halogens) maintained activity. The 3,4-dichloro and 3,4-difluoro were notable exceptions, with > 10-fold loss of activity. In

Table 1
SAR of the amide portion of compound, **3.**

Cmpd	Structure	GIRK1/2 (nM ± SEM[a]; % ± SEM[b])	GIRK1/4 (nM ± SEM[a]; % ± SEM[b])
3	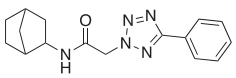	1983 ± 546; 13 ± 1	2761 ± 753; 7 ± 1
15a	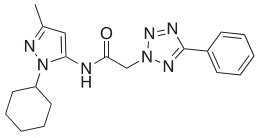	96 ± 7; 92 ± 2	259 ± 25; 63 ± 2
15b	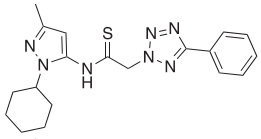	623 ± 72; 80 ± 3	1256 ± 92; 36 ± 1
15c	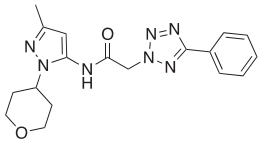	435 ± 22; 115 ± 2	2,037 ± 114; 109 ± 3
15d	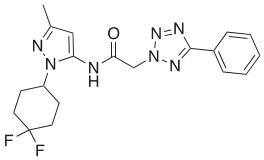	84 ± 9; 68 ± 2	383 ± 36; 52 ± 2
15e	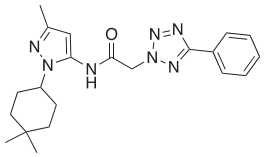	> 221; > 19	Inactive
15f	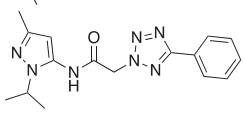	556 ± 55; 107 ± 3	> 4000; > 96
15g	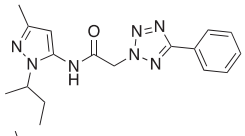	> 5000; > 69	> 10,000; > 20
15h	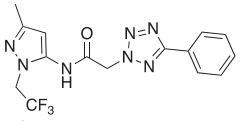	> 6000; > 105	> 10,000; > 97
15i	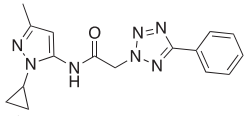	> 5000; > 78	> 10,000; > 39
15j	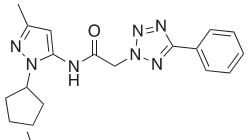	163 ± 7; 105 ± 1	612 ± 32; 84 ± 2
15k	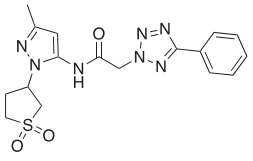	1034 ± 66; 93 ± 1	2168 ± 172; 75 ± 2

Table 1 (*continued*)

Cmpd	Structure	GIRK1/2 (nM ± SEM[a]; % ± SEM[b])	GIRK1/4 (nM ± SEM[a]; % ± SEM[b])
15l	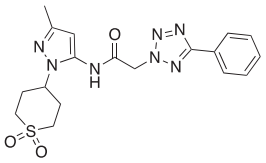	> 10,000; > 25	Inactive
15m	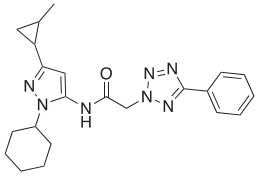	843 ± 139; 78 ± 4	> 10,000; > 19
15n	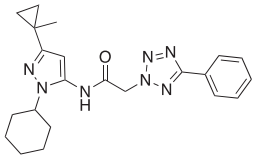	> 10,000; > 10	Inactive
15o	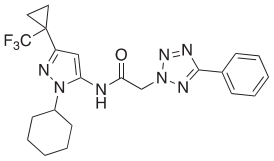	Inactive	Inactive
15p	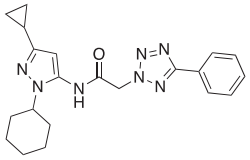	271 ± 17; 45 ± 1	659 ± 57; 15 ± 0
15q	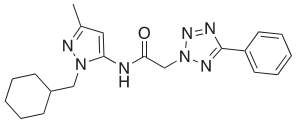	176 ± 16; 77 ± 2	283 ± 26; 58 ± 2
15r	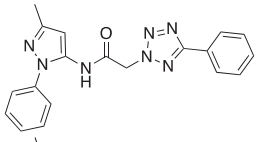	3019 ± 517; 66 ± 3	4093 ± 528; 25 ± 1
15s	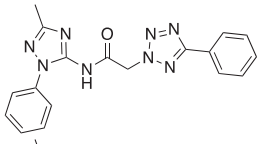	Inactive	Inactive
15t	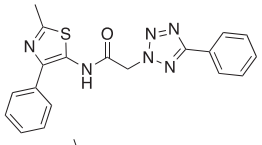	Inactive	Inactive
15u	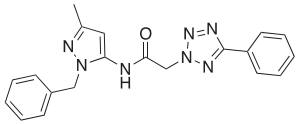	495 ± 75; 74 ± 2	848 ± 121; 48 ± 2
15v	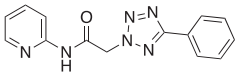	Inactive	Inactive

[a] Potency values were obtained from triplicate determinations; values are average of n = 3.

[b] Reported efficacy values shown are obtained from triplicate determinations; values are average of n = 3 and are normalized to standard compound, VU0466551.

Table 2

SAR of the tetrazole substituent.

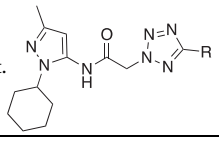

Cmpd	Structure	GIRK1/2 (nM ± SEM[a]; % ± SEM[b])	GIRK1/4 (nM ± SEM[a];% ± SEM[b])
16a		1931 ± 89; 96 ± 1	4908 ± 165; 80 ± 1
16b		14,571 ± 1379; 81 ± 3	> 33,000; > 41
16c		300 ± 29; 89 ± 2	662 ± 75; 66 ± 2
16d	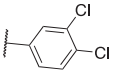	1217 ± 91; 84 ± 2	2201 ± 130; 70 ± 1
16e	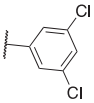	980 ± 68; 82 ± 1	2122 ± 331; 51 ± 2
16f	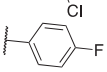	180 ± 11; 92 ± 1	634 ± 45; 74 ± 2
16g		81 ± 7; 96 ± 2	264 ± 22; 80 ± 2
16h		187 ± 22; 88 ± 3	447 ± 42; 60 ± 2
16i	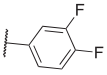	116 ± 6; 93 ± 1	392 ± 23; 79 ± 2
16j		441 ± 57; 95 ± 4	1,337 ± 181; 68 ± 4
16k		> 3000; > 83	> 10,000; > 38
16l	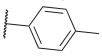	111 ± 9; 86 ± 2	408 ± 29; 64 ± 1
16m		129 ± 15; 93 ± 3	435 ± 113; 63 ± 6
16n	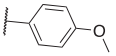	175 ± 13; 90 ± 1	779 ± 78; 65 ± 1
16o	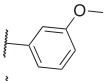	117 ± 9; 76 ± 2	299 ± 18; 40 ± 1
16p		> 3000; > 68	> 10,000; > 25
16q	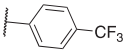	241 ± 11; 94 ± 1	448 ± 39; 50 ± 1
16r	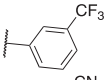	183 ± 17; 86 ± 2	850 ± 200; 57 ± 4
16s	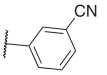	183 ± 18; 80 ± 2	619 ± 80; 55 ± 3
16t	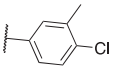	712 ± 25; 89 ± 1	1510 ± 89; 51 ± 1

[a] Potency values were obtained from triplicate determinations; values are average of n = 3.

[b] Reported efficacy values shown are obtained from triplicate determinations; values are average of n = 3 and are normalized to standard compound, VU0466551.

addition, the fluoro substituted compounds were more active than the chloro substitutions (e.g., **16g**, EC_{50} = 81 nM, vs. **16c**, EC_{50} = 300 nM, and **16i**, EC_{50} = 116 nM, vs. **16d**, EC_{50} = 1218 nM). Although these compounds were potent and efficacious against GIRK1/2, they did not impart selectivity versus GIRK1/4 (only approximately 3–5-fold selective). The 2-fluoro-4-pyridyl analog maintained potency (**16j**, EC_{50} = 441 nM); however, the 2-fluoro-6-pyridyl analog was much less potent (**16k**, EC_{50} = > 3000 nM). Other substituents that were well tolerated and generated active compounds included alkyl, methoxy, trifluoromethyl, and cyano (**16l–s**). The cycloalkyl substituents appear to be poorly tolerated (**16p**); however, we only investigated a small sample size.

Table 3

Aryl and heterocyclic replacements.

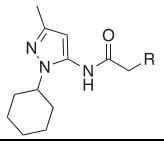

Cmpd	Structure	GIRK1/2 (nM ± SEM[a]; % ± SEM[b])	GIRK1/4 (nM ± SEM[a]; % ± SEM[b])
17a	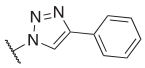	116 ± 3; 87 ± 1	412 ± 26; 76 ± 1
17b	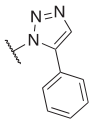	375 ± 33; 87 ± 2	1027 ± 85; 49 ± 1
17c	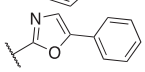	631 ± 154; 72 ± 5	1132 ± 79; 27 ± 1
17d	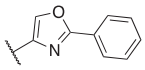	> 11,000; > 69	3979 ± 547; 22 ± 1
17e	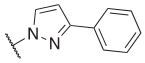	511 ± 29; 88 ± 2	998 ± 105; 49 ± 2
17f	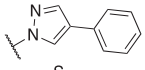	65 ± 6; 72 ± 2	348 ± 15; 52 ± 1
17g	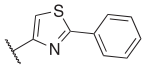	1326 ± 227; 44 ± 3	> 3000; > 18
17h	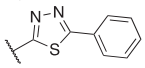	> 3000; > 60	> 10,000; > 21
17i	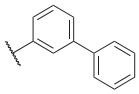	370 ± 95; 72 ± 5	> 4000; > 51
17j	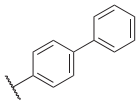	1657 ± 297; 69 ± 6	1825 ± 424; 20 ± 2
17k	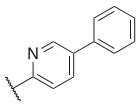	1520 ± 115; 36 ± 1	Inactive
17l	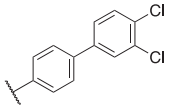	4471 ± 318; 49 ± 2	4352 ± 326; 11 ± 1

[a] Potency values were obtained from triplicate determinations; values are average of n = 3.

[b] Reported efficacy values shown are obtained from triplicate determinations; values are average of n = 3 and are normalized to standard compound, VU0466551.

Finally, we explored aryl and heterocyclic replacements for the tetrazole moiety (Table 3). Replacing the tetrazole with the triazole led to two regioisomers (**17a**, **b**). The 4-substituted triazole was more active (**17a**, EC_{50} = 116 nM); however, the 5-substituted analog did retain some potency (**17b**, EC_{50} = 375 nM). The 5-phenyloxazol-2-ylacetic acid derivative (**17c**, EC_{50} = 631 nM) was much more potent than the

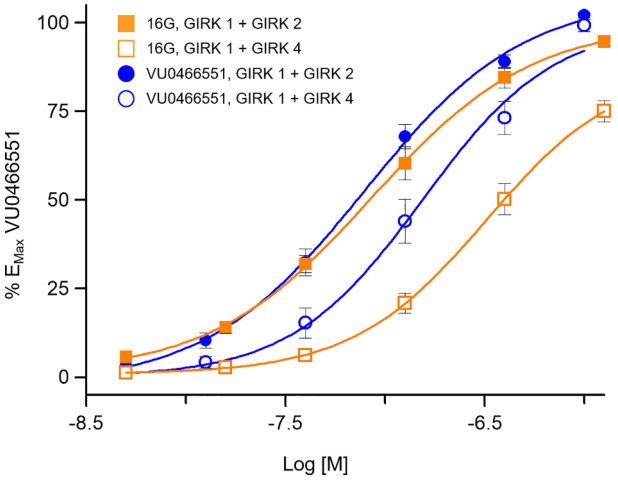

Fig. 2. Activation CRC's for VU0466551, **1** and **16g**.

2-phenyloxazol-4-ylacetic acid analog (**17d**, EC_{50} = > 11,000 nM). Although, the oxazole was much less active than the tetrazole or triazole. Further exploration of the regio-chemistry of the nitrogens and determination of whether these atoms were necessary led us to the pyrazole derivatives (**17e**, **f**). Interestingly, we identified a distinct regioisomeric requirement for potency. The 3-phenyl-1*H*-pyrazole, **17e**, was ~8-fold less potent than the 4-phenyl-1*H*-pyrazole, **17f** (EC_{50} = 511 nM vs. EC_{50} = 65 nM). The nitrogen placement in the 4-phenyl-1*H*-pyrazole maintained the nitrogen in a similar arrangement as the triazole (**17a**) and the original tetrazole (**15a**). Thiazole, **17g**, and thiadiazole, **17h**, did not maintain potency, and this can be explained by the position of the nitrogen/sulfur in the thiazole and the increased ring size in the thiadiazole (or due to the presence of the sulfur atom, in general). The *meta*-phenyl substituted analog possessed moderate activity (**17i**, EC_{50} = 370 nM); however, all of the *para*-substituted analogs were less active (**17j–l**).

The thallium flux data resulting from the treatment of GIRK1/2 or GIRK1/4 expressing cells with an activator (**1** or **16g**) is shown in Fig. 2. As can be seen, both **1** and **16g** activate GIRK1/2 preferentially over GIRK1/4; however, **16g** is more selective for GIRK1/2 vs. GIRK1/4 when compared to **1**. The $\%E_{max}$ has been normalized to the standard compound, **1**. Data are the average of three independent determinations. Error bars represent the standard error of the mean (SEM).

Having established a robust SAR for this new scaffold of GIRK1/2 activators, we next evaluated select compounds in a panel of Tier 1 *in vitro* DMPK assays (Table 4, Q2 Solutions, Indianapolis, IN).[22,23] Unfortunately, all of the compounds tested were unstable in both human and mouse liver microsomes, with the singular exception of **15k**. This compound was unique in that it possessed the cyclic five-membered sulfone moiety on the pyrazolo head group. Compound **15k** was stable in both human and mouse liver microsomes and was stable in human S9 fractions.[24,25] In addition to displaying excellent stability in liver microsomes, **15k**, also showed increased free fraction in human plasma (% f_u = 3.7). Unfortunately, this improvement in stability did not include an increase in potency as **15k** was much less potent (EC_{50} = 1034 nM). Curiously, all of the compounds tested had poor recovery in mouse plasma, leading us to theorize that the compounds were unstable due to the amidases present in plasma.[26] Several compounds were made to test this hypothesis (thioamide, **15b**, amide *N*-methylation, and α-carbon methylation). However, all of these compounds also showed poor recovery in mouse plasma (data not shown).

In conclusion, we have identified a novel series of 5-aryl-2*H*-tetrazol-3-ylacetamides as GIRK1/2 channel activators. This series was born out of an HTS hit molecule. SAR around the initial head group found that the pyrazolo privileged group was optimal. Further SAR identified the optimal tetrazole substituent as well as heterocyclic replacements. These compounds were found to be unstable in liver microsomes as well as mouse plasma, with the one exception being the cyclic five-membered sulfone derivative. Although the *in vitro* DMPK profile of these compounds are less than ideal, our discovery of these compounds increases the number of potent, efficacious, and modestly-selective GIRK1/2 channel activators from a novel scaffold, and these compounds will add to the armament of GIRK channel researchers. Further work and evaluation of lead molecules is ongoing and will be reported in due course.

Acknowledgments

The authors would like to thank Q2 solutions for the *in vitro* DMPK experiments. The study was supported by a grant from the NIH (NIMH: R01MH107399) to C.R.H. and C.D.W. C.D.W. is an owner of WaveFront

Table 4
In vitro Tier 1 DMPK of select compounds.

Cmpd	Intrinsic Clearance (mL/min/kg)[a,b]				Plasma unbound ($\%f_u$)[a,c]	
	hCL_{INT}	hCL_{HEP}	mCL_{INT}	mCL_{HEP}	Human	Mouse
15a	186.5	18.9	2917.5	87.0	1.1	*
15b	346.5	18.9	> 5930	> 88.7	< 0.06	*
15d	77.3	15.9	722.7	80.0	1.5	*
15k	< 23.1	< 10.7	< 49.5	< 31.9	3.7	*
15q	753.1	20.4	> 5930	88.7	0.3	*
16d	99.9	17.4	489.1	76.0	< 0.3	*
16g	162.4	17.8	2710.6	87.1	1.0	*
17a	54.6	14.6	596.0	78.2	3.0	*
17b	209.1	18.3	3487.8	87.7	0.4	*
Stability in Human Liver S9 fractions						
	$T_{1/2}$ (min)	CL_{INT} (mL/min/kg)		CL_{HEP} (mL/min/kg)		ER[c]
15k	647.5	2.6		< 1.0		< 0.05

[a] *In vitro* DMPK studies performed at Q2 Solutions, Indianapolis, IN
[b] Intrinsic and predicted hepatic clearance based on experiments in liver microsomes. [b]$\%f_u$ = % fraction unbound.
[c] ER = extraction ratio and defines the % of drug amount eliminated by the liver from the incoming blood supply in every pass through the liver (0 not eliminated by liver, 100 completely eliminated by liver).
* Poor recovery.

Biosciences, maker of the Panoptic kinetic imaging plate reader used in these studies.

Appendix A. Supplementary data

Supplementary data to this article can be found online at https://doi.org/10.1016/j.bmcl.2019.01.027.

References

1. Dascal N. *Cell Sig.* 1997;9:551.
2. Yamada M, Inanobe A, Kurachi Y. *Pharmacol Rev.* 1998;50:723.
3. Aryal P, Dvir H, Choe S, Slesinger PA. *Nat Neurosci.* 2009;12:988.
4. Hibino H, Inanobe A, Furutani K, Murakami S, Findlay I, Kurachi Y. *Physiol Rev.* 2010;90:291.
5. Lyu C, Mulder J, Barde S, et al. *Mol Pain.* 2015;11:44.
6. Bruehl S, Denton JS, Lonergan DF, et al. *Pain.* 2013;154:2853.
7. Nishizawa D, Fukuda K, Kasai S, et al. *J Pharmacol Sci.* 2014;126:253.
8. Kaufmann K, Romaine I, Days E, et al. *ACS Chem Neurosci.* 2013;4:1278.
9. Luján R, Fernandez de Velasco EM, Aguado C, Wickman K. *Trends Pharmacol Sci.* 2014;37:20.
10. Wydeven N, Fernandez de Velasco EM, Du Y, et al. *Proc Natl Acad Sci USA.* 2014;111:10755.
11. Sánchez-Rodríguez I, Temprano-Carazo S, Nájera A, et al. *Sci Rep.* 2017;7:14658.
12. Fernandez de Velasco EM, McCall N, Wickman K. *Int Rev Neurobiol.* 2015;123:201.
13. Rifkin RA, Moss SJ, Slesinger PA. *Trends Pharmacol Sci.* 2017;38:378.
14. Sugaya N, Kobayashi T, Ikeda KJ. *Drug Alc Res.* 2013;2:235823.
15. Wieting JM, Vadukoot AK, Sharma S, et al. *ACS Chem Neurosci.* 2017:8.
16. Ramos-Hunter SJ, Engers DW, Kaufmann K, et al. *Bioorg Med Chem Lett.* 2013;23:5195.
17. Wen W, Wu W, Weaver CD, Lindsley CW. *Bioorg Med Chem Lett.* 2014;24:5102.
18. Akkari, R.; Alvey, L. J.; Bock, X. M.; Brown, B. S.; Claes, P. I. R.; Cowart, M. D.; De Lemos, E.; Desroy, N.; Duthion, B.; Gfesser, G. A.; Gosmini, R. L. M.; Housseman, C. G.; Jansen, K. K.; Ji, J.; Kym, P. R.; Lefrancois, J.-M.; Mamoliti, O.; Menet, C. J. M.; Merayo, N. M.; Newsome, G. J. R.; Palisse, A. M. E.; Patel, S. V.; Pizzonero, M. R.; Shrestha, A.; Swift, E. C.; Van der Plas, S. E.; Wang, X.; De Blieck, A. US2017/0101405, 2017.
19. Koguro K, Oga T, Mitsui S, Orita R. *Synthesis.* 1998:910.
20. Maxwell JR, Wasdahl DA, Wolfson A, Stenberg VI. *J Med Chem.* 1984;27:1565.
21. Vishwanatha BTM, Panguluri NR, Sureshbabu VV. *Synthesis.* 2013;45:1569.
22. Chang G, Steyn SJ, Umland JP, Scott DO. *ACS Med Chem Lett.* 2010;1:50.
23. Liu X, Wright M, Hop CECA. *J Med Chem.* 2014;57:8238.
24. Richardson SJ, Bai A, Kulkami AA, Moghaddam MF. *Drug Metab Lett.* 2016;10:83.
25. Gautam N, Bathena SP, Chen Q, Natarajan A, Alnouti Y. *Biomed Chromatogr.* 2013;27:900.
26. Teffera Y, Berry LM, Brake RL, et al. *Drug Metab Dispos.* 2013;41:238.